

CE-LoRA: Computation-Efficient LoRA Fine-Tuning for Language Models

Guanduo Chen^{*†}
Fudan University
gdchen22@m.fudan.edu.cn

Yutong He[†]
Peking University
yutonghe@pku.edu.cn

Yipeng Hu
Peking University
yipenghu@pku.edu.cn

Kun Yuan[‡]
Peking University
kunyuan@pku.edu.cn

Binhang Yuan[‡]
HKUST
biyuan@ust.hk

Abstract

Large Language Models (LLMs) demonstrate exceptional performance across various tasks but demand substantial computational resources even for fine-tuning computation. Although Low-Rank Adaptation (LoRA) significantly alleviates memory consumption during fine-tuning, its impact on computational cost reduction is limited. This paper identifies the computation of activation gradients as the primary bottleneck in LoRA’s backward propagation and introduces the **Computation-Efficient LoRA (CE-LoRA)** algorithm, which enhances computational efficiency while preserving memory efficiency. CE-LoRA leverages two key techniques: Approximated Matrix Multiplication, which replaces dense multiplications of large and complete matrices with sparse multiplications involving only critical rows and columns, and the Double-LoRA technique, which reduces error propagation in activation gradients. Theoretically, CE-LoRA converges at the same rate as LoRA, $\mathcal{O}(1/\sqrt{T})$, where T is the number of iterations. Empirical evaluations confirm that CE-LoRA significantly reduces computational costs compared to LoRA without notable performance degradation.

1 Introduction

Large Language Models (LLMs) have garnered significant attention in recent years for their exceptional performance across a wide range of practical tasks, including machine translation, common-sense reasoning, and planning, among others [1]. The versatility of these models has also driven a growing demand for fine-tuning them on specific tasks or domains to unlock their full potential [2, 3]. However, fine-tuning these models remains a highly resource-intensive process, demanding substantial computational power and large amounts of GPU memory. As model parameters and training tokens scale up, the increasing training costs have made it difficult for most organizations to keep pace with advancements in LLM research due to resource constraints.

To tackle these challenges, recent advancements such as Low-Rank Adaptation (LoRA) [4] have demonstrated promising results in reducing memory consumption during LLM fine-tuning, enabling the fine-tuning of models with more parameters or larger batch sizes within constrained resources. While LoRA significantly alleviates memory requirements, its reduction of computational costs remains limited — although the low-rank adapters can save part of the computation costs by reducing the matrix sizes, the size of original weight matrices used to calculate *activation gradients* remains unchanged, which contributes to half of the total computation cost in the backpropagation of the original model. The formulation of this computation is illustrated in Section 2. Limited by this computational bottleneck, LoRA can reduce computation by at most half during the backpropagation process. This limitation raises the following open question:

* Work done when the author was working as a research assistant under the supervision of Binhang Yuan.

† Both authors contributed equally to this research.

‡ Coresponding author.

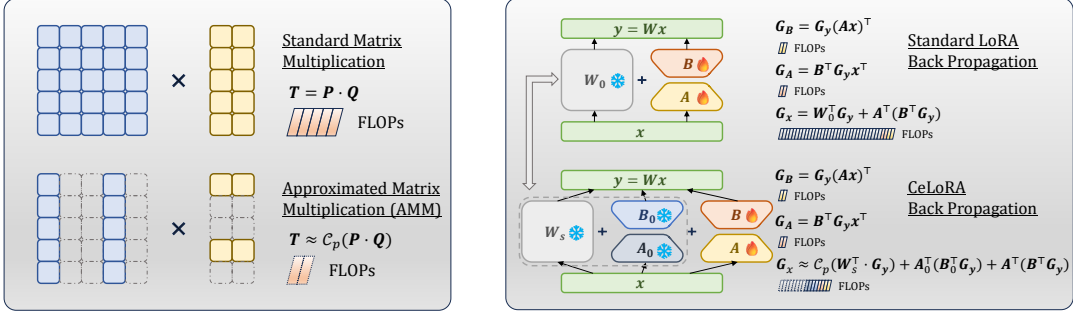


Figure 1: An illustration of the Approximated Matrix Multiplication (AMM) technique (left) and the CE-LoRA framework (right).

Compared with vanilla LoRA, can we develop a more computation-efficient fine-tune algorithm by the same memory budget without sacrificing the statistical efficiency (i.e., convergence)?

To answer this question, we first conduct a computational analysis of LoRA’s backward propagation procedure and identify the primary computational bottleneck as the *calculation of the activation gradients*. This step accounts for the majority of the backward computation load, especially when LoRA employs a relatively small rank r .

Based on this analysis, we propose the Approximated Matrix Multiplication (AMM) technique to reduce the computation of activation gradients. In order to reduce the computation of a dense matrix multiplication $T = P Q$, where $P \in \mathbb{R}^{m \times n}$ and $Q \in \mathbb{R}^{n \times k}$, AMM directly reduces the size of the matrices by discarding unimportant rows or columns, obtaining $P[:, \mathcal{I}]$ and $Q[\mathcal{I}, :]$, as illustrated in Figure 1 (left). Compared to the original multiplication procedure, AMM reduces the computational complexity to $|\mathcal{I}|/n$ times by instead multiplying $P[:, \mathcal{I}]$ with $Q[\mathcal{I}, :]$, trading computational accuracy for computational efficiency. To identify the important rows or columns, we compute the importance scores $\alpha_i = \|P[:, i] Q[i, :]\|_F$ every τ iterations and select the top ones in the following τ times of AMM operation.

Unfortunately, the computational error in the activations’ gradients can further propagate to previous layers. Under such a long-lasting effect of inaccurate activation gradients, the accumulated computational error can lead to poor gradient estimations, which severely harms the optimization procedure and degrades the final model performance. To resolve this issue, we develop a double-LoRA technique that significantly reduces the relative error induced to the activation gradients by AMM. Specifically, double-LoRA splits the frozen dense weight matrix into two parts, where the first part applies AMM to save computation, the second part is a frozen LoRA adapter which is computation-efficient without using AMM. In order to reduce the AMM-induced error, we expect the first part to include as little information as possible. Consequently, we initially conduct SVD of the parameter matrix and identify the first part according to the smallest singular values and corresponding vectors. Combining the above techniques, we propose **Computation-Efficient LoRA (CE-LoRA)**, which is more computation-efficient and equally memory-efficient compared with LoRA.

We evaluate the proposed CE-LoRA algorithm both theoretically and empirically. In theory, we prove that CE-LoRA with momentum SGD converges at a rate of $\mathcal{O}(1/\sqrt{T})$, the same order of LoRA’s convergence rate. Empirically, we validate that CE-LoRA can converge at a comparable precision as standard LoRA, with slightly reduced memory consumption and a $3.39\times$ acceleration in computation. To our knowledge, CE-LoRA is the *first* algorithm that accelerates LoRA without sacrificing memory-efficiency or leading to notable performance degradation.

The main contributions of this paper are as follows:

- We propose a novel algorithm CE-LoRA, which is more computation-efficient and equally memory-efficient compared with standard LoRA.
- We theoretically prove that CE-LoRA converges at a rate of $\mathcal{O}(1/\sqrt{T})$, which is the same order of standard LoRA’s convergence rate.

- We experimentally validate that CE-LoRA has a 3.39 \times acceleration compared with LoRA without sacrificing memory-efficiency or leading to notable training performance degradation.

2 Preliminaries

2.1 LoRA Algorithm

In order to fine-tune language models memory-efficiently, LoRA applies a low-rank adapter to each linear layer in the model. Specifically, let $\mathbf{y} = \mathbf{W}\mathbf{x}$ represent a linear layer with $\mathbf{y} \in \mathbb{R}^{m \times b}$, $\mathbf{W} \in \mathbb{R}^{m \times n}$ and $\mathbf{x} \in \mathbb{R}^{n \times b}$, where m, n represent the output and input dimension, respectively, and b represents the batch-size. The LoRA adapter is given by $\mathbf{W} = \mathbf{W}_0 + \mathbf{B}\mathbf{A}$ with $\mathbf{W}_0 \in \mathbb{R}^{m \times n}$ fixed as the pre-trained weights, $\mathbf{B} \in \mathbb{R}^{m \times r}$ and $\mathbf{A} \in \mathbb{R}^{r \times n}$ trainable.

$$\mathbf{y} = \mathbf{W}\mathbf{x}, \quad (\text{Original})$$

$$\mathbf{y} = (\mathbf{W}_0 + \mathbf{B}\mathbf{A})\mathbf{x}. \quad (\text{LoRA})$$

When $r \ll \min\{m, n\}$, the number of trainable parameters in LoRA, $(m + n)r$, is much fewer than that in full fine-tuning, *i.e.*, mn , which significantly reduces the memory consumption of the optimizer states.

2.2 Computational Bottleneck

While applying LoRA can significantly reduce the memory cost for fine-tuning large language models, the computational cost for computing the gradient via back propagation is not sufficiently reduced. Specifically, let \mathbf{G}_θ denote the stochastic gradient of θ calculated by back propagation, for linear layer $\mathbf{y} = \mathbf{W}\mathbf{x}$ we compute:

$$\mathbf{G}_\mathbf{W} = \mathbf{G}_\mathbf{y} \cdot \mathbf{x}^\top, \quad (1)$$

$$\mathbf{G}_\mathbf{x} = \mathbf{W}^\top \cdot \mathbf{G}_\mathbf{y}, \quad (2)$$

Both (1) and (2) require $2bmn$ FLOPs of computation. Accordingly, in LoRA we compute:

$$\mathbf{G}_\mathbf{B} = \mathbf{G}_\mathbf{y} \cdot \mathbf{z}^\top, \quad (3)$$

$$\mathbf{G}_\mathbf{z} = \mathbf{B}^\top \cdot \mathbf{G}_\mathbf{y}, \quad (4)$$

$$\mathbf{G}_\mathbf{A} = \mathbf{G}_\mathbf{z} \cdot \mathbf{x}^\top, \quad (5)$$

$$\mathbf{G}_{\mathbf{x},1} = \mathbf{A}^\top \cdot \mathbf{G}_\mathbf{z}, \quad (6)$$

$$\mathbf{G}_{\mathbf{x},2} = \mathbf{W}_0^\top \cdot \mathbf{G}_\mathbf{y}, \quad (7)$$

$$\mathbf{G}_\mathbf{x} = \mathbf{G}_{\mathbf{x},1} + \mathbf{G}_{\mathbf{x},2}, \quad (8)$$

where $\mathbf{z} = \mathbf{A}\mathbf{x} \in \mathbb{R}^{r \times b}$ represents LoRA's additional activation. (3)(4)(5)(6)(7)(8) require $2brm$, $2brm$, $2brn$, $2brn$, $2bmn$, and bn FLOPs of computation, respectively, resulting in $4br(m + n) + 2bmn + bn$ FLOPs in total. When $r \ll \min\{m, n\}$, the computational cost in LoRA's back propagation is roughly $2bmn$, half of the computation in the original approach (1)(2). The computational bottleneck lies in the dense matrix multiplication step in (7), which alone requires $2bmn$ FLOPs of computation.

3 CE-LoRA: Computation-Efficient LoRA

3.1 Approximated Matrix Multiplication (AMM)

Consider matrix multiplication $\mathbf{T} = \mathbf{P}\mathbf{Q}$, where $\mathbf{T} \in \mathbb{R}^{m \times k}$, $\mathbf{P} \in \mathbb{R}^{m \times n}$ and $\mathbf{Q} \in \mathbb{R}^{n \times k}$. Let $\mathbf{p}_1, \mathbf{p}_2, \dots, \mathbf{p}_n$ denote the column vectors of matrix \mathbf{P} , and $\mathbf{q}_1, \mathbf{q}_2, \dots, \mathbf{q}_n$ denote the column vectors of matrix \mathbf{Q}^\top . We can rewrite the matrix multiplication into:

$$\mathbf{T} = \sum_{i=1}^n \mathbf{p}_i \mathbf{q}_i^\top.$$

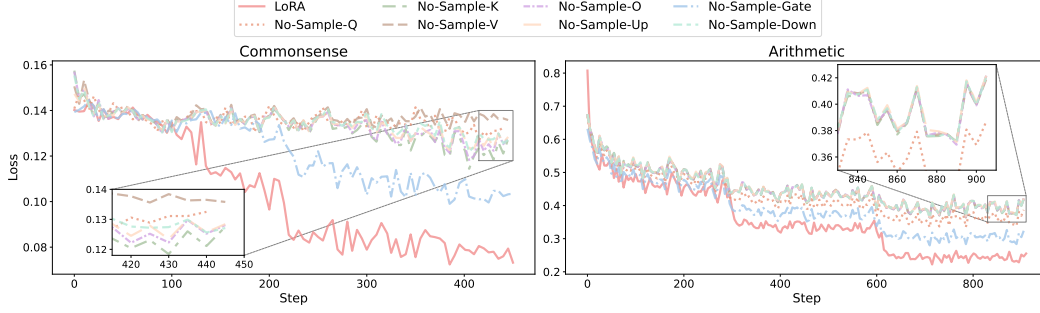


Figure 2: Layer-wise Sensitivity Analysis of LLaMA3.2-1B.

To estimate the product \mathbf{T} computation-efficiently, we may assume the matrices \mathbf{P} and \mathbf{Q} enjoy some kinds of structured sparsity, such that a few $(\mathbf{p}_i \mathbf{q}_i^\top)$'s contribute to most of the result $\sum_{i=1}^n \mathbf{p}_i \mathbf{q}_i^\top$, in which case we could estimate \mathbf{T} by computing the most important parts only. Specifically, we identify s most important indices $1 \leq i_1 < \dots < i_s \leq n$, and the AMM estimate of \mathbf{T} is given by:

$$\hat{\mathbf{T}} = \sum_{j=1}^s \mathbf{p}_{i_j} \mathbf{q}_{i_j}^\top = \hat{\mathbf{P}} \hat{\mathbf{Q}},$$

where $\hat{\mathbf{P}}$ and $\hat{\mathbf{Q}}^\top$ collect column vectors $\{\mathbf{p}_{i_j}\}_{j=1}^s$ and $\{\mathbf{q}_{i_j}\}_{j=1}^s$, respectively.

The efficiency of AMM is concerned with the number of selected indices s , or the structured sparsity $p := s/n \in (0, 1]$. Replacing the dense matrix multiplication $\mathbf{T} = \mathbf{P}\mathbf{Q}$ by AMM estimate $\hat{\mathbf{T}} = \hat{\mathbf{P}}\hat{\mathbf{Q}}$, the computational complexity is reduced from $2mnk$ to $2msk = p \cdot (2mnk)$. Hereafter, we use $\mathcal{C}_p(\mathbf{P} \cdot \mathbf{Q})$ to denote the AMM estimate of matrix multiplication $\mathbf{P} \cdot \mathbf{Q}$ with structured sparsity p .

An important question is how to select the indices $\mathcal{I} = \{i_1, i_2, \dots, i_s\}$ properly. A previous research [5] has studied a random sampling strategy, which does not work well in our experiments. Based on the above intuition, we define the importance score α_i of index i by the Frobenius norm $\|\mathbf{p}_i \mathbf{q}_i^\top\|_F$ and attempt to select the indices with highest scores. However, as calculating $\{\alpha_i\}_{i=1}^k$ requires the same amount of computation as that of conducting the original matrix multiplication, we cannot determine \mathcal{I} based on the calculation results of $\{\alpha_i\}_{i=1}^k$ in every iteration. We use historical information to mitigate this issue. Specifically, the matrices \mathbf{P}, \mathbf{Q} we multiply by AMM should be variables that live along the whole optimization process, and $\mathbf{P}^t, \mathbf{Q}^t$ are multiplied at every iteration t . The corresponding \mathcal{I}^t is only re-selected according to the top- s importance scores every τ iterations and is reused in intermediate ones.

To reduce the computational bottleneck in LoRA's backward propagation, we apply AMM to step (7) and get:

$$\mathbf{G}_{\mathbf{x},2} = \mathcal{C}_p(\mathbf{W}_0^\top \cdot \mathbf{G}_{\mathbf{y}}). \quad (9)$$

3.2 Double-LoRA Mechanism

Although computation-efficient, AMM will induce errors to g_x , the gradient with respect to the activations. These errors propagate backward through the network, potentially compounding as they traverse previous layers. If the magnitude of these errors is not properly controlled, the accuracy of the parameter gradients can be significantly degraded. To mitigate this issue, we propose a double-LoRA mechanism to alleviate the error induced by the AMM operation in each layer. Intuitively, we wish the objective matrix multiplication result we estimate by AMM has as little contribution to the activation gradient as possible. This drives us to further separate the frozen matrix \mathbf{W}_0 into two parts: a low-rank part inheriting computational efficiency without AMM, and a residual part with a relatively small magnitude.

Specifically, we initially compute the SVD of \mathbf{W}_0 , yielding

$$\mathbf{W}_0 = \mathbf{U}\mathbf{\Sigma}\mathbf{V}^\top$$

Next, We collect the principal low-rank r component $\mathbf{B}_0 = \mathbf{U}[:, r]\mathbf{\Sigma}^{1/2}$, $\mathbf{A}_0 = \mathbf{\Sigma}^{1/2}(\mathbf{V}[:, r])^\top$, and the residual $\mathbf{W}_s = \mathbf{W}_0 - \mathbf{B}_0\mathbf{A}_0$. By separating \mathbf{W}_0 to $\mathbf{W}_s + \mathbf{B}_0\mathbf{A}_0$, we split the matrix to two

Algorithm 1 CE-LoRA

Input: Frozen layer weight $\mathbf{W}_\ell \in \mathbb{R}^{m_\ell \times n_\ell}$, sparsity level p_ℓ , double-LoRA rank $r_{0,\ell}$, indices recomputing period τ , Top-K indices $\mathcal{I}_\ell = \text{empty}$, optimizer ρ .

Initialize Double-LoRA

- 1: **for** Layer $\ell = 1, 2, \dots, L$ **do**
- 2: Conducting SVD on frozen weight matrix
 $\mathbf{W}_{0,\ell} = \mathbf{U}_\ell \mathbf{\Sigma}_\ell \mathbf{V}_\ell^\top$;
- 3: $\mathbf{A}_{0,\ell}, \mathbf{B}_{0,\ell} \leftarrow \sqrt{\mathbf{\Sigma}_\ell} \mathbf{V}_\ell^\top_{[:,r_{0,\ell}]}, \mathbf{U}_{\ell[:,r_{0,\ell}]} \sqrt{\mathbf{\Sigma}_\ell}$; ▷ Stored in layer’s buffer.
- 4: **end for**

5: **for** CE-LoRA Training Step $t = 0, 1, \dots, T - 1$ **do**

- 6: **for** Layer $\ell = 1, 2, \dots, L$ **do** ▷ **Forward**
- 7: $\mathbf{z}_\ell \leftarrow \mathbf{A}_\ell \mathbf{x}_\ell$;
- 8: $\mathbf{y}_\ell \leftarrow \mathbf{W}_{0,\ell} \mathbf{x}_\ell + \mathbf{B}_\ell \mathbf{z}_\ell$;
- 9: **end for**
- 10: **for** Layer $\ell = L, L - 1, \dots, 1$ **do** ▷ **Backward**
- 11: $\mathbf{W}_{s,\ell} \leftarrow \mathbf{W}_{0,\ell} - \mathbf{B}_{0,\ell} \mathbf{A}_{0,\ell}$;
- 12: **if** $\tau \mid t$ or \mathcal{I}_ℓ is empty **then**
- 13: $\alpha_{i,\ell} \leftarrow \left\| \mathbf{W}_{s,\ell}^\top_{s,\ell[:,i]} \mathbf{G}_{\mathbf{y}_\ell} [i,:] \right\|_F, \forall i \in \{1, \dots, m_\ell\}$
- 14: Select $\{i_{1,\ell}, \dots, i_{K_\ell,\ell}\}$ with largest $\alpha_{i,\ell}$ ’s;
- 15: $\mathcal{I}_\ell = \{i_{1,\ell}, \dots, i_{K_\ell,\ell}\}$; ▷ Here $K_\ell = \lceil m_\ell p_\ell \rceil$
- 16: **end if**
- 17: $\mathbf{G}_{\mathbf{B}_\ell} \leftarrow \mathbf{G}_{\mathbf{y}_\ell} \mathbf{z}_\ell^\top$;
- 18: $\mathbf{G}_{\mathbf{z}_\ell} \leftarrow \mathbf{B}_\ell^\top \mathbf{G}_{\mathbf{y}_\ell}$;
- 19: $\mathbf{G}_{\mathbf{A}_\ell} \leftarrow \mathbf{G}_{\mathbf{z}_\ell} \mathbf{x}_\ell^\top$;
- 20: $\mathbf{G}_{\mathbf{x}_\ell} \leftarrow \mathbf{W}_{s,\ell}^\top_{s,\ell[\mathcal{I},\cdot]} \mathbf{G}_{\mathbf{y}_\ell} [\mathcal{I},\cdot] + \mathbf{A}_{0,\ell}^\top (\mathbf{B}_{0,\ell}^\top \mathbf{G}_{\mathbf{y}_\ell}) + \mathbf{A}_\ell^\top \mathbf{G}_{\mathbf{z}_\ell}$;
- 21: **end for**
- 22: Use optimizer ρ to update $\{\mathbf{A}_\ell, \mathbf{B}_\ell\}_{\ell=1}^L$ according to $\{\mathbf{G}_{\mathbf{A}_\ell}, \mathbf{G}_{\mathbf{B}_\ell}\}_{\ell=1}^L$;
- 23: **end for**

parts. The first part \mathbf{W}_s is believed to have better structured sparsity and is more compatible to AMM. The second low-rank part $\mathbf{B}_0 \mathbf{A}_0$ is computation-efficient just like the trainable LoRA adapter $\mathbf{B}\mathbf{A}$. Combining AMM with double-LoRA, (9) is further replaced by

$$\mathbf{G}_{\mathbf{x},2} = \mathcal{C}_p(\mathbf{W}_s^\top \cdot \mathbf{G}_{\mathbf{y}}) + \mathbf{A}_0^\top (\mathbf{B}_0^\top \mathbf{G}_{\mathbf{y}}). \quad (10)$$

3.3 Layer-wise Adaptive Sparsity

It is natural to apply more aggressive sparsity to layers that are relatively robust to computational errors, while using more conservative sparsity for those that are more sensitive. Inspired by [6–12], we adopt a layer-wise adaptive sparsity strategy for CE-LoRA.

To determine which layers are more sensitive to varying sparsity levels, we conduct experiments on two small fine-tuning datasets: the Commonsense 14K dataset and the Math 7K dataset [13]. In these experiments, we fix LoRA’s rank to 32, and set both CE-LoRA’s trainable LoRA rank and its frozen Double-LoRA rank to 28. For each CE-LoRA configuration, we vary the sparsity level of one layer type, while setting the sparsity of all remaining layer types to $p = 0.3$. As shown in Figure 2, the Gate layers are essential for preventing error propagation. In addition, the Q and K layers have a strong impact on arithmetic and commonsense reasoning tasks, respectively. Based on these findings, we disable sparsity for the Q, K, and Gate layers. For the remaining MHA layers, we use $p = 0.55$, and for the last two layers in the FFN, we set $p = 0.65$ throughout our experiments.

3.4 Algorithm

Overall, CE-LoRA integrates AMM, double-LoRA, and layer-wise adaptivity, as outlined in Algorithm 1. During model initialization, we replace all frozen linear layers with CE-LoRA and apply the double-LoRA technique to the weight matrix \mathbf{W}_0 , resulting in low-rank components \mathbf{A}_0 and \mathbf{B}_0 (lines 2–3). For each training step t , the forward pass of a CE-LoRA linear layer behaves the same as

the original frozen linear layer (lines 8). In the backward pass, CE-LoRA first computes the residual weight matrix by subtracting the low-rank components from the original weight matrix (line 11). Next, if the current step t is a multiple of τ or if the indices are empty (e.g., at the start of training), the top-K indices are updated (lines 12–15). Finally, CE-LoRA uses AMM to compute activation gradient $\mathbf{G}_{\mathbf{x}_\ell}$ (line 20).

3.5 Complexity Analysis

To better illustrate the computational efficiency of CE-LoRA, we theoretically compare the computational and memory complexity of CE-LoRA with LoRA and standard AdamW fine-tuning. Consider linear layer $\mathbf{y} = \mathbf{W}\mathbf{x}$ with $\mathbf{W} \in \mathbb{R}^{m \times n}$, trained with LoRA rank r , double-LoRA rank r_0 , structured sparsity p and batch size b using BF16 precision. As illustrated in Table 1, CE-LoRA can achieve a memory usage similar to LoRA by applying slightly smaller r_0 and r , while significantly reduce the backward computation by applying a relatively small p when $b \gg 1$ and $r \ll \min\{m, n\}$. When combined with low-precision training, the influence of double-LoRA can be further reduced, as the frozen low-rank parameters do not require high-precision weight copies or gradient accumulators.

4 Convergence Analysis

We first present the assumptions under which we prove CE-LoRA’s convergence properties.

Assumption 4.1 (Lower Boundedness). The loss function $f : \mathbb{R}^d \rightarrow \mathbb{R}$ satisfies $\inf_{\mathbf{x} \in \mathbb{R}^d} f(\mathbf{x}) > -\infty$.

Assumption 4.2 (L -Smoothness). The loss function f is L -smooth, i.e., it holds for any $\mathbf{x}, \mathbf{y} \in \mathbb{R}^d$ that

$$\|\nabla f(\mathbf{x}) - \nabla f(\mathbf{y})\|_2 \leq L\|\mathbf{x} - \mathbf{y}\|_2.$$

Assumption 4.3 (Stochastic Gradient). We assume the stochastic gradient oracle satisfies

$$\mathbb{E}[\nabla F(\mathbf{x}^t; \xi^t)] = \nabla f(\mathbf{x}^t); \tag{11}$$

$$\mathbb{E}[\|\nabla F(\mathbf{x}^t; \xi^t) - \nabla f(\mathbf{x}^t)\|^2] \leq \sigma^2, \tag{12}$$

for some $\sigma > 0$.

Assumptions 4.1-4.3 are standard assumptions commonly used in stochastic optimization.

Assumption 4.4 (Gradient Error). Let \mathbf{g}^t and $\hat{\mathbf{g}}^t$ denote the original stochastic gradient $\nabla F(\mathbf{x}^t, \xi^t)$ and its estimation by CE-LoRA, it holds that

$$\|\hat{\mathbf{g}}^t - \mathbf{g}^t\|^2 \leq (1 - \delta)\|\mathbf{g}^t\|^2, \tag{13}$$

and

$$\|\mathbb{E}_{\xi^t \sim \mathcal{D}}[\hat{\mathbf{g}}^t] - \nabla f(\mathbf{x}^t)\|^2 \leq (1 - \delta)\|\nabla f(\mathbf{x}^t)\|^2, \tag{14}$$

for some $\delta \in (0, 1]$.

Assumption 4.4 illustrates the property of stochastic gradients in CE-LoRA. Though not standard, this assumption can be empirically justified by our experimental results.

Table 1: Computation and memory analysis for a single linear layer.

| Method | Standard AdamW | LoRA | CE-LoRA |
|-----------------------------|----------------|--------------------------------|--|
| Memory Usage | $10mn + 2bm$ | $2mn + 10r(m + n) + 2b(m + r)$ | $2mn + 2r_0(m + n) + 10r(m + n) + 2b(m + r)$ |
| Forward Computation | $2bmn$ | $2bmn + 2br(m + n)$ | $2bmn + 2br(m + n)$ |
| Backward Computation | $4bmn$ | $2bmn + 4br(m + n)$ | $(2pb + 1)mn + 2(r_0 + br_0 + 2br)(m + n)$ |

Empirical Justification of Assumption 4.4. To justify (13), we conduct experiments on language model fine-tuning tasks on google/gemma-2b [14] model using CoLA [15], RTE and MRPC [16] datasets, three tasks in the GLUE benchmark [17]. In these experiments, we use AdamW with a learning rate of $1e-5$ to train for 1 epoch per task and calculate the relative error $\|\hat{\mathbf{g}}^t - \mathbf{g}^t\|^2 / \|\mathbf{g}^t\|^2$ every 10 steps, as illustrated in Figure 3, where all relative errors are below 0.9. To justify (14), we conduct experiments on the same model and datasets, where we alternatively calculate one iteration of full gradient AdamW and one epoch of random gradient AdamW, each with a learning rate of $1e-5$ for a total of 80 cycles. We apply a rank of 64 for both LoRA and double-LoRA in CE-LoRA, and apply a structured sparsity of $p_{\text{FFN}} = 0.9$ and $p_{\text{MHA}} = 0.4$. We calculate the relative error $\|\mathbb{E}_{\xi^t \sim \mathcal{D}}[\hat{\mathbf{g}}^t] - \nabla f(\mathbf{x}^t)\|^2 / \|\nabla f(\mathbf{x}^t)\|^2$ for every full-gradient step, as illustrated in Figure 4, where all relative errors are below 0.9.

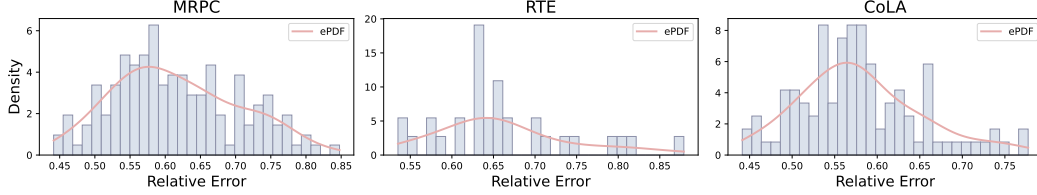


Figure 3: Empirical validation of (13) on MRPC (left), RTE (middle) and CoLA (right).

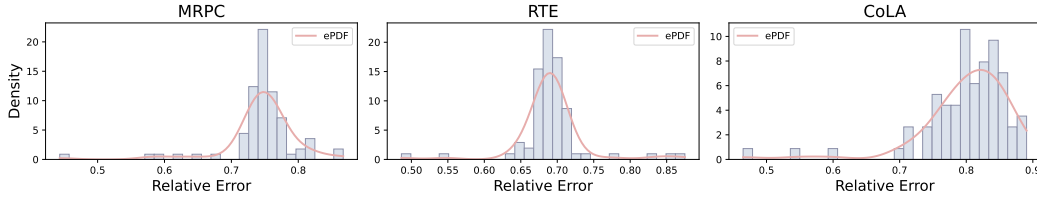


Figure 4: Empirical validation of (14) on MRPC (left), RTE (middle) and CoLA (right).

We now propose the convergence results of CE-LoRA using the momentum SGD optimizer with the following update:

$$\begin{aligned} \mathbf{m}^t &= (1 - \beta_1)\mathbf{m}^{t-1} + \beta_1\hat{\mathbf{g}}^t, \\ \mathbf{x}^{t+1} &= \mathbf{x}^t - \eta\mathbf{m}^t, \end{aligned}$$

Theorem 4.5. Under Assumptions 4.1 - 4.4, if $\beta_1 \in \left(0, \frac{\delta}{24-12\delta}\right)$ and $\eta \leq \min\left\{\frac{L}{2}, \frac{\beta_1}{L} \cdot \sqrt{\frac{\delta}{8}}\right\}$, CE-LoRA with momentum SGD converges as

$$\frac{1}{T+1} \sum_{t=0}^T \mathbb{E}[\|\nabla f(\mathbf{x}^t)\|_2^2] \leq \frac{4[f(\mathbf{x}^0) - \inf_{\mathbf{x}} f(\mathbf{x})]}{\delta\eta(T+1)} + \frac{4\|\mathbf{m}^0 - \nabla f(\mathbf{x}^0)\|_2^2}{\delta\beta_1(T+1)} + \frac{12\beta_1\sigma^2}{\delta}.$$

Corollary 4.6. Under Assumptions 4.1-4.4, if we choose $\beta_1 = \left(\frac{24}{\delta} + \sigma\sqrt{\frac{\delta^{1/2}(T+1)}{L\Delta}}\right)^{-1}$, $\eta = \left(2L + \frac{2^{3/2}L}{\delta^{1/2}\beta_1}\right)^{-1}$, CE-LoRA with momentum SGD converges as

$$\frac{1}{T+1} \sum_{t=0}^T \mathbb{E}[\|\nabla f(\mathbf{x}^t)\|_2^2] = \mathcal{O}\left(\frac{L\Delta}{\delta^{5/2}(T+1)} + \sqrt{\frac{L\Delta\sigma^2}{\delta^{5/2}(T+1)}}\right),$$

where $\Delta := f(\mathbf{x}^0) - \inf_{\mathbf{x}} f(\mathbf{x}) + (\delta/L) \cdot \|\mathbf{m}^0 - \nabla f(\mathbf{x}^0)\|_2^2$.

Detailed proofs are deferred to Appendix A.

5 Experiments

In this section, we present a comprehensive set of experiments to evaluate the convergence performance and computational efficiency of CE-LoRA, and compare it against the baseline method.

5.1 Experimental Setup

Datasets. We follow the benchmark design outlined in [13] and evaluate CE-LoRA on two popular reasoning benchmarks:

- **Commonsense Reasoning:** This dataset includes eight tasks: BoolQ [18], PIQA [19], SocialQA [20], HellaSwag [21], WinoGrande [22], ARC-challenge [23], ARC-easy [23], and OpenbookQA [24]. In our experiments, we fine-tune all models using the Commonsense 170K dataset [13], which is constructed by combining the training sets from these eight tasks.
- **Arithmetic Reasoning:** This benchmark consists of seven subsets: MultiArith [25], GSM8K [26], AddSub [27], AQuA [28], SingleEq [29], SVAMP [30] and MAWPS [31]. We fine-tune the models on the Math 10k dataset [13], which includes training data from GSM8K, MAWPS, and AQuA, augmented by language models with chain-of-thought reasoning steps.

Fine-tuned models and hyper-parameters. We fine-tune LLaMA-2-7B, LLaMA-2-13B [32], and LLaMA-3.1-8B [33] using both CE-LoRA and LoRA. The adapter is applied to all linear layers in each transformer block, including Q, K, V, O, Up, Gate, and Down. Unless specified otherwise, all CE-LoRA experiments replace the frozen V, O, Up, and Down layers with CE-LoRA layers. The sparsity levels are set as follows: $p_V = p_O = 0.55$ and $p_{Up} = p_{Down} = 0.65$. For consistency, the same set of hyperparameters is applied across both methods for each model size. All experiments are conducted using the BF16 format to optimize memory usage.

5.2 Statistical Efficiency of CE-LoRA

In this set of experiments, we evaluate the convergence performance of CE-LoRA using two critical metrics: the accuracy achieved on each benchmark and the trajectory of the fine-tuning loss across training iterations. By monitoring these metrics, we aim to gain insights into how quickly and effectively CE-LoRA converges compared to LoRA.

Accuracy. We trained both CE-LoRA and LoRA under low-rank (LoRA rank of 16, CE-LoRA rank of 14) and high-rank (LoRA rank of 64, CE-LoRA rank of 56) configurations across two reasoning datasets for one epoch. Table 2 and Table 3 summarize the results for the commonsense and arithmetic reasoning benchmarks. The experimental outcomes demonstrate that, across all LoRA rank settings in both benchmarks, CE-LoRA achieves fine-tuning accuracy that is nearly identical to that of LoRA, with an average difference in results of 1.58%. These findings suggest that our approach has a negligible impact on the original LoRA fine-tuning accuracy. The slight differences in accuracy between CE-LoRA and LoRA on the test sets can primarily be attributed to the scaling of CE-LoRA’s rank, which was adjusted to ensure a fair experimental comparison.

Table 2: Comparison among eight commonsense reasoning tasks for the LLaMA2-7B/13B, LLaMA3.1-8B models

| Model | Method | Rank | BoolQ | PIQA | SIQA | HellaSwag | Wino | ARC-e | ARC-c | OBQA | Avg. \uparrow |
|------------|---------|------|-------|-------|-------|-----------|-------|-------|-------|-------|-----------------|
| LLaMA2-7B | LoRA | 16 | 71.99 | 84.49 | 81.73 | 94.45 | 85.95 | 87.63 | 73.21 | 83.80 | 82.91 |
| | CE-LoRA | 14 | 70.24 | 82.59 | 79.27 | 93.17 | 82.72 | 85.56 | 70.65 | 79.80 | 80.50 |
| | LoRA | 64 | 72.26 | 84.88 | 82.70 | 94.97 | 86.42 | 88.55 | 74.74 | 86.40 | 83.87 |
| | CE-LoRA | 56 | 71.68 | 85.20 | 82.09 | 94.61 | 83.98 | 87.29 | 73.29 | 84.20 | 82.79 |
| LLaMA2-13B | LoRA | 16 | 75.32 | 88.03 | 83.21 | 81.14 | 92.34 | 88.20 | 96.08 | 88.71 | 86.63 |
| | CE-LoRA | 14 | 73.21 | 86.62 | 82.14 | 94.65 | 86.27 | 90.15 | 77.22 | 84.80 | 84.38 |
| | LoRA | 64 | 75.72 | 88.85 | 84.39 | 96.34 | 88.71 | 92.42 | 81.83 | 89.60 | 87.23 |
| | CE-LoRA | 56 | 74.01 | 86.51 | 83.11 | 92.74 | 87.92 | 91.37 | 79.61 | 85.40 | 85.08 |
| LLaMA3-8B | LoRA | 16 | 75.84 | 90.86 | 83.52 | 96.93 | 89.90 | 94.07 | 84.47 | 88.8 | 88.05 |
| | CE-LoRA | 14 | 72.08 | 89.72 | 82.65 | 96.24 | 88.32 | 93.35 | 83.36 | 87.60 | 86.66 |
| | LoRA | 64 | 75.63 | 90.21 | 83.32 | 96.38 | 88.95 | 93.39 | 84.04 | 89.20 | 87.64 |
| | CE-LoRA | 56 | 73.36 | 89.66 | 82.40 | 95.76 | 86.42 | 93.14 | 82.68 | 87.60 | 86.38 |

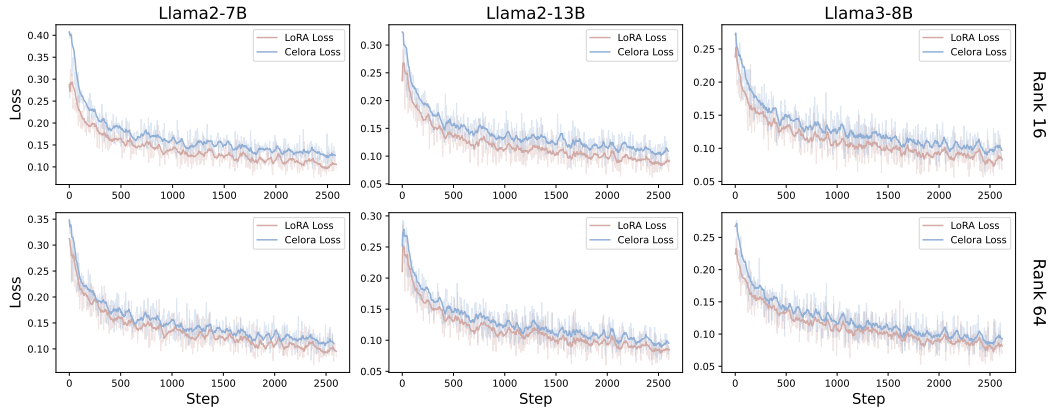


Figure 5: Loss curve of commonsense reasoning fine-tune task. Each row in the figure corresponds to a different trainable parameter setting, while each column represents base models: LLaMA2-7B/13B and LLaMA3.1-8B.

Loss curve. Figure 5 illustrates the loss curves of both CE-LoRA and LoRA under different rank settings across the three models on the commonsense reasoning fine-tuning task. In each setting, CE-LoRA’s loss curves nearly overlap with those of its LoRA counterparts, indicating similar convergence behaviors. These results highlight the effectiveness of our method, empirically demonstrating that CE-LoRA can achieve nearly the same convergence capability as the original LoRA while potentially offering computational savings. The overlapping loss curves suggest that CE-LoRA does not introduce additional convergence challenges and maintains training stability comparable to LoRA.

5.3 Computation Efficiency

In these experiments, we measure CE-LoRA’s training efficiency by comparing the average training step latency of a single-layer CE-LoRA with a single-layer LoRA. All experiments are conducted on a single NVIDIA-HGX-H20- (96GB) GPU to maintain consistent hardware conditions. For a fair comparison, both CE-LoRA and LoRA employ the same trainable rank of 64. We run experiments on three different model weight sizes—(8192, 8192), (4096, 4096), and (2048, 2048)—using a fixed batch size of 16 and a sequence length of 8192. To measure average training step latency, each configuration is tested over 100 runs. The first 10 iterations of each run are considered warmup and are excluded from latency measurements to mitigate initialization overhead.

Figure 6 compares the results of LoRA and CE-LoRA with various sparsity levels and shows that CE-LoRA achieves a consistent reduction in overall training time, with a maximum of 36.3% speedup. As illustrated, CE-LoRA’s forward pass latency closely matches that of LoRA’s due to the unchanged forward logic of the frozen layer. However, in the backward pass, CE-LoRA outperforms LoRA by up to $3.39\times$ with some aggressive sampling rate. The observed improvements in wall-clock speed are primarily attributed to two key factors: (i) CE-LoRA effectively reduces the theoretical floating-point operations required during backpropagation for frozen layers. (ii) We developed specialized CUDA kernels tailored for low-rank computations inherent in CE-LoRA’s backpropagation process, which optimize memory access patterns, resulting in enhanced computational efficiency and reduced latency.

Table 3: Performance comparison of LoRA and CE-LoRA on seven arithmetic reasoning tasks.

| Model | Method | Rank | MultiArith | GSM8K | AddSub | AQuA | SingleEq | SVAMP | MAWPS | Avg. \uparrow |
|-----------|---------|------|------------|-------|--------|-------|----------|-------|-------|-----------------|
| LLaMA3-8B | LoRA | 16 | 94.50 | 64.59 | 90.89 | 47.24 | 92.13 | 76.30 | 88.66 | 79.19 |
| | CE-LoRA | 14 | 94.00 | 62.09 | 91.14 | 44.88 | 93.50 | 75.00 | 90.76 | 78.77 |
| | LoRA | 64 | 96.33 | 65.50 | 90.63 | 49.61 | 92.91 | 81.2 | 89.50 | 80.81 |
| | CE-LoRA | 56 | 96.17 | 62.02 | 88.86 | 47.64 | 93.31 | 77.10 | 89.08 | 79.17 |

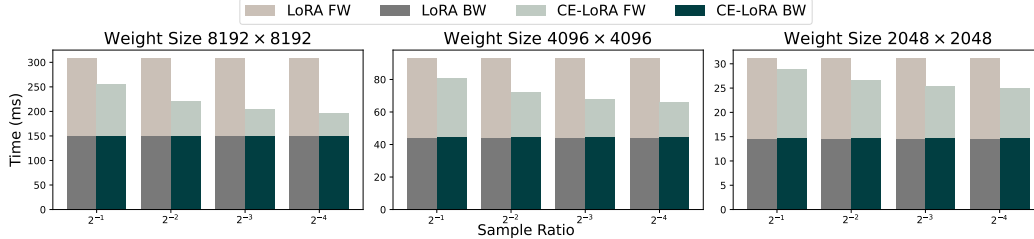


Figure 6: Comparison of training latency for CE-LoRA and LoRA at various sparsity levels (i.e., $\frac{1}{2}$, $\frac{1}{4}$, $\frac{1}{8}$, $\frac{1}{16}$) across three model shapes: (8192, 8192), (4096, 4096), and (2048, 2048). CE-LoRA provides significant speedups in the backward pass, leading to a maximum of 36.3% overall reduction in end-to-end training time compared to LoRA.

6 Related Works

Large Language Models. Since the transformer structure was proposed in the famous work [34] in 2017, it has shown great potential in various tasks, including reasoning, planning, machine translation, *etc.*, and has become a popular choice in modern LLM designs, *e.g.*, GPT [35–37], OPT [38], LLaMA [39–41], BLOOM [42], BERT [43], Falcon [44], *etc.* In general, the basic structure of a transformer block consists of a multi-head attention (MHA) module followed by a feed-forward network (FFN), combined with normalization and residual connections. Linear layers take up most of the trainable parameters in transformers and account for the expensive training and inference costs.

Memory-Efficient Training Algorithms. As the scale of LLM parameters grows, the memory consumption to train these models has become a bottleneck problem. Recent studies have proposed a series of works in order to reduce training-time memory consumption, enabling LLM researchers to effectively pre-train / fine-tune larger LLMs within constrained computational resources. [45, 46] fine-tune LLMs parameter-efficiently by adding trainable adapter layers, LoRA [4] reparameterizes linear layers in transformers with low-rank adapters, ReLoRA [47] extends to pre-training tasks by accumulating LoRA updates, S²FT [48] applies sparse structures, SLTrain [49] combines low-rank and sparse structures. Besides the above parameter-efficient approaches, another line of works reduce the memory consumption for optimizer states by optimizing in periodically updated subspaces, including LISA [50], GaLore [51], GoLore [52] and FLORA [53]. In addition, BackRazor [54] and PreBackRazor [55] improve memory-efficiency by compressing the activation memory. Furthermore, quantization methods [56, 57] that are orthogonal to the above approaches have shown nice compatibilities in memory cost reduction.

Computation-Efficient Training Algorithms. Though not specially designed for computational efficiency, a lot of memory-efficient training algorithms, particularly those belong to parameter-efficient fine-tuning (PEFT), can also reduce computational costs to some extent. On the other hand, the training throughput can also be improved by utilizing a larger batch size thanks to the reduced memory consumption [58]. However, the computational savings of these approaches are limited by precisely retaining the complete backward propagation process. Recently, [59] proposes DropBP, an approach orthogonal to PEFT that saves computation by strategically skip connections in backward propagation. Since some layers are dropped during backward propagation, corresponding parameters do not have gradients for update. To the best of our knowledge, this paper provides the *first* approach to accelerate LoRA by employing structured sparsity to reduce the computational bottleneck in backward propagation without sacrificing memory-efficiency or model performance.

7 Conclusion

We propose CE-LoRA that saves computational FLOPs by approximated matrix multiplication and controls the compression error by a novel double LoRA technique and layer-wise compression ratios. While enjoying a 3.39 times of acceleration compared to LoRA, CE-LoRA theoretically converges at a rate of $\mathcal{O}(1/\sqrt{T})$ and shows comparable performance in our experiments.

References

- [1] Rishi Bommasani, Drew A Hudson, Ehsan Adeli, Russ Altman, Simran Arora, Sydney von Arx, Michael S Bernstein, Jeannette Bohg, Antoine Bosselut, Emma Brunskill, et al. On the opportunities and risks of foundation models. *arXiv preprint arXiv:2108.07258*, 2021.
- [2] Shengyu Zhang, Linfeng Dong, Xiaoya Li, Sen Zhang, Xiaofei Sun, Shuhe Wang, Jiwei Li, Runyi Hu, Tianwei Zhang, Fei Wu, et al. Instruction tuning for large language models: A survey. *arXiv preprint arXiv:2308.10792*, 2023.
- [3] Zeyu Han, Chao Gao, Jinyang Liu, Jeff Zhang, and Sai Qian Zhang. Parameter-efficient fine-tuning for large models: A comprehensive survey. *arXiv preprint arXiv:2403.14608*, 2024.
- [4] Edward J Hu, Yelong Shen, Phillip Wallis, Zeyuan Allen-Zhu, Yuanzhi Li, Shean Wang, Lu Wang, and Weizhu Chen. Lora: Low-rank adaptation of large language models. *arXiv preprint arXiv:2106.09685*, 2021.
- [5] Petros Drineas, Ravi Kannan, and Michael W Mahoney. Fast monte carlo algorithms for matrices i: Approximating matrix multiplication. *SIAM Journal on Computing*, 36(1):132–157, 2006.
- [6] Gansen Hu, Zhaoguo Wang, Jinglin Wei, Wei Huang, and Haibo Chen. Accelerating large language models through partially linear feed-forward network. *arXiv e-prints*, pages arXiv–2501, 2025.
- [7] Chi Ma, Mincong Huang, Ying Zhang, Chao Wang, Yujie Wang, Lei Yu, Chuan Liu, and Wei Lin. First activations matter: Training-free methods for dynamic activation in large language models. *arXiv preprint arXiv:2408.11393*, 2024.
- [8] Ajay Jaiswal, Lu Yin, Zhenyu Zhang, Shiwei Liu, Jiawei Zhao, Yuandong Tian, and Zhangyang Wang. From galore to welore: How low-rank weights non-uniformly emerge from low-rank gradients. *arXiv preprint arXiv:2407.11239*, 2024.
- [9] Binrui Zeng, Bin Ji, Xiaodong Liu, Jie Yu, Shasha Li, Jun Ma, Xiaopeng Li, Shangwen Wang, and Xinran Hong. Lsaq: Layer-specific adaptive quantization for large language model deployment. *arXiv preprint arXiv:2412.18135*, 2024.
- [10] Vladimir Malinovskii, Andrei Panferov, Ivan Ilin, Han Guo, Peter Richtárik, and Dan Alistarh. Pushing the limits of large language model quantization via the linearity theorem. *arXiv preprint arXiv:2411.17525*, 2024.
- [11] Zhenyu Zhang, Ajay Jaiswal, Lu Yin, Shiwei Liu, Jiawei Zhao, Yuandong Tian, and Zhangyang Wang. Q-galore: Quantized galore with int4 projection and layer-adaptive low-rank gradients. *arXiv preprint arXiv:2407.08296*, 2024.
- [12] James Liu, Pragaash Ponnusamy, Tianle Cai, Han Guo, Yoon Kim, and Ben Athiwaratkun. Training-free activation sparsity in large language models. *arXiv preprint arXiv:2408.14690*, 2024.
- [13] Zhiqiang Hu, Yihuai Lan, Lei Wang, Wanyu Xu, Ee-Peng Lim, Roy Ka-Wei Lee, Lidong Bing, and Soujanya Poria. Llm-adapters: An adapter family for parameter-efficient fine-tuning of large language models. *arXiv preprint arXiv:2304.01933*, 2023.
- [14] google/gemma-2b.
- [15] Alex Warstadt, Amanpreet Singh, and Samuel R. Bowman. Neural network acceptability judgments. *Transactions of the Association for Computational Linguistics*, 7:625–641, 2019.
- [16] William B. Dolan and Chris Brockett. Automatically constructing a corpus of sentential paraphrases. In *Proceedings of the Third International Workshop on Paraphrasing (IWP2005)*, 2005.
- [17] Alex Wang, Amanpreet Singh, Julian Michael, Felix Hill, Omer Levy, and Samuel R. Bowman. Glue: A multi-task benchmark and analysis platform for natural language understanding, 2019.

- [18] Christopher Clark, Kenton Lee, Ming-Wei Chang, Tom Kwiatkowski, Michael Collins, and Kristina Toutanova. BoolQ: Exploring the surprising difficulty of natural yes/no questions. In Jill Burstein, Christy Doran, and Thamar Solorio, editors, *Proceedings of the 2019 Conference of the North American Chapter of the Association for Computational Linguistics: Human Language Technologies, Volume 1 (Long and Short Papers)*, pages 2924–2936, Minneapolis, Minnesota, June 2019. Association for Computational Linguistics.
- [19] Yonatan Bisk, Rowan Zellers, Jianfeng Gao, Yejin Choi, et al. Piqa: Reasoning about physical commonsense in natural language. In *Proceedings of the AAAI conference on artificial intelligence*, volume 34, pages 7432–7439, 2020.
- [20] Maarten Sap, Hannah Rashkin, Derek Chen, Ronan LeBras, and Yejin Choi. Socialliqa: Commonsense reasoning about social interactions. *arXiv preprint arXiv:1904.09728*, 2019.
- [21] Rowan Zellers, Ari Holtzman, Yonatan Bisk, Ali Farhadi, and Yejin Choi. Hellaswag: Can a machine really finish your sentence? *arXiv preprint arXiv:1905.07830*, 2019.
- [22] Keisuke Sakaguchi, Ronan Le Bras, Chandra Bhagavatula, and Yejin Choi. Winogrande: An adversarial winograd schema challenge at scale. *Communications of the ACM*, 64(9):99–106, 2021.
- [23] Peter Clark, Isaac Cowhey, Oren Etzioni, Tushar Khot, Ashish Sabharwal, Carissa Schoenick, and Oyvind Tafjord. Think you have solved question answering? try arc, the ai2 reasoning challenge. *arXiv preprint arXiv:1803.05457*, 2018.
- [24] Todor Mihaylov, Peter Clark, Tushar Khot, and Ashish Sabharwal. Can a suit of armor conduct electricity? a new dataset for open book question answering. *arXiv preprint arXiv:1809.02789*, 2018.
- [25] Subhro Roy and Dan Roth. Solving general arithmetic word problems. *arXiv preprint arXiv:1608.01413*, 2016.
- [26] Karl Cobbe, Vineet Kosaraju, Mohammad Bavarian, Mark Chen, Heewoo Jun, Lukasz Kaiser, Matthias Plappert, Jerry Tworek, Jacob Hilton, Reiichiro Nakano, et al. Training verifiers to solve math word problems. *arXiv preprint arXiv:2110.14168*, 2021.
- [27] Mohammad Javad Hosseini, Hannaneh Hajishirzi, Oren Etzioni, and Nate Kushman. Learning to solve arithmetic word problems with verb categorization. In *Proceedings of the 2014 Conference on Empirical Methods in Natural Language Processing (EMNLP)*, pages 523–533, 2014.
- [28] Wang Ling, Dani Yogatama, Chris Dyer, and Phil Blunsom. Program induction by rationale generation: Learning to solve and explain algebraic word problems. In Regina Barzilay and Min-Yen Kan, editors, *Proceedings of the 55th Annual Meeting of the Association for Computational Linguistics (Volume 1: Long Papers)*, pages 158–167, Vancouver, Canada, July 2017. Association for Computational Linguistics.
- [29] Rik Koncel-Kedziorski, Hannaneh Hajishirzi, Ashish Sabharwal, Oren Etzioni, and Siena Dumas Ang. Parsing algebraic word problems into equations. *Transactions of the Association for Computational Linguistics*, 3:585–597, 2015.
- [30] Arkil Patel, Satwik Bhattamishra, and Navin Goyal. Are NLP models really able to solve simple math word problems? In Kristina Toutanova, Anna Rumshisky, Luke Zettlemoyer, Dilek Hakkani-Tur, Iz Beltagy, Steven Bethard, Ryan Cotterell, Tanmoy Chakraborty, and Yichao Zhou, editors, *Proceedings of the 2021 Conference of the North American Chapter of the Association for Computational Linguistics: Human Language Technologies*, pages 2080–2094, Online, June 2021. Association for Computational Linguistics.
- [31] Rik Koncel-Kedziorski, Subhro Roy, Aida Amini, Nate Kushman, and Hannaneh Hajishirzi. MAWPS: A math word problem repository. In Kevin Knight, Ani Nenkova, and Owen Rambow, editors, *Proceedings of the 2016 Conference of the North American Chapter of the Association for Computational Linguistics: Human Language Technologies*, pages 1152–1157, San Diego, California, June 2016. Association for Computational Linguistics.

- [32] Hugo Touvron, Louis Martin, Kevin Stone, Peter Albert, Amjad Almahairi, Yasmine Babaei, Nikolay Bashlykov, Soumya Batra, Prajjwal Bhargava, Shruti Bhosale, Dan Bikel, Lukas Blecher, Cristian Canton Ferrer, Moya Chen, Guillem Cucurull, David Esiobu, Jude Fernandes, Jeremy Fu, Wenyin Fu, Brian Fuller, Cynthia Gao, Vedanuj Goswami, Naman Goyal, Anthony Hartshorn, Saghar Hosseini, Rui Hou, Hakan Inan, Marcin Kardas, Viktor Kerkez, Madian Khabsa, Isabel Kloumann, Artem Korenev, Punit Singh Koura, Marie-Anne Lachaux, Thibaut Lavril, Jenya Lee, Diana Liskovich, Yinghai Lu, Yuning Mao, Xavier Martinet, Todor Mihaylov, Pushkar Mishra, Igor Molybog, Yixin Nie, Andrew Poulton, Jeremy Reizenstein, Rashi Rungta, Kalyan Saladi, Alan Schelten, Ruan Silva, Eric Michael Smith, Ranjan Subramanian, Xiaoqing Ellen Tan, Binh Tang, Ross Taylor, Adina Williams, Jian Xiang Kuan, Puxin Xu, Zheng Yan, Iliyan Zarov, Yuchen Zhang, Angela Fan, Melanie Kambadur, Sharan Narang, Aurelien Rodriguez, Robert Stojnic, Sergey Edunov, and Thomas Scialom. Llama 2: Open foundation and fine-tuned chat models, 2023.
- [33] AI@Meta. Llama 3 model card. 2024.
- [34] A Vaswani. Attention is all you need. *Advances in Neural Information Processing Systems*, 2017.
- [35] Alec Radford. Improving language understanding by generative pre-training. 2018.
- [36] Alec Radford, Jeffrey Wu, Rewon Child, David Luan, Dario Amodei, Ilya Sutskever, et al. Language models are unsupervised multitask learners. *OpenAI blog*, 1(8):9, 2019.
- [37] Tom Brown, Benjamin Mann, Nick Ryder, Melanie Subbiah, Jared D Kaplan, Prafulla Dhariwal, Arvind Neelakantan, Pranav Shyam, Girish Sastry, Amanda Askell, et al. Language models are few-shot learners. *Advances in neural information processing systems*, 33:1877–1901, 2020.
- [38] Susan Zhang, Stephen Roller, Naman Goyal, Mikel Artetxe, Moya Chen, Shuohui Chen, Christopher Dewan, Mona Diab, Xian Li, Xi Victoria Lin, et al. Opt: Open pre-trained transformer language models. *arXiv preprint arXiv:2205.01068*, 2022.
- [39] Hugo Touvron, Thibaut Lavril, Gautier Izacard, Xavier Martinet, Marie-Anne Lachaux, Timothée Lacroix, Baptiste Rozière, Naman Goyal, Eric Hambro, Faisal Azhar, et al. Llama: Open and efficient foundation language models. *arXiv preprint arXiv:2302.13971*, 2023.
- [40] Hugo Touvron, Louis Martin, Kevin Stone, Peter Albert, Amjad Almahairi, Yasmine Babaei, Nikolay Bashlykov, Soumya Batra, Prajjwal Bhargava, Shruti Bhosale, et al. Llama 2: Open foundation and fine-tuned chat models. *arXiv preprint arXiv:2307.09288*, 2023.
- [41] Abhimanyu Dubey, Abhinav Jauhri, Abhinav Pandey, Abhishek Kadian, Ahmad Al-Dahle, Aiesha Letman, Akhil Mathur, Alan Schelten, Amy Yang, Angela Fan, et al. The llama 3 herd of models. *arXiv preprint arXiv:2407.21783*, 2024.
- [42] Teven Le Scao, Angela Fan, Christopher Akiki, Ellie Pavlick, Suzana Ilić, Daniel Hesslow, Roman Castagné, Alexandra Sasha Luccioni, François Yvon, Matthias Gallé, et al. Bloom: A 176b-parameter open-access multilingual language model. 2023.
- [43] Jacob Devlin. Bert: Pre-training of deep bidirectional transformers for language understanding. *arXiv preprint arXiv:1810.04805*, 2018.
- [44] Guilherme Penedo, Quentin Malartic, Daniel Hesslow, Ruxandra Cojocaru, Alessandro Cappelli, Hamza Alobeidli, Baptiste Pannier, Ebtesam Almazrouei, and Julien Launay. The refinedweb dataset for falcon llm: outperforming curated corpora with web data, and web data only. *arXiv preprint arXiv:2306.01116*, 2023.
- [45] Neil Houlsby, Andrei Giurgiu, Stanislaw Jastrzebski, Bruna Morrone, Quentin De Laroussilhe, Andrea Gesmundo, Mona Attariyan, and Sylvain Gelly. Parameter-efficient transfer learning for nlp. In *International conference on machine learning*, pages 2790–2799. PMLR, 2019.
- [46] Jonas Pfeiffer, Andreas Rücklé, Clifton Poth, Aishwarya Kamath, Ivan Vulić, Sebastian Ruder, Kyunghyun Cho, and Iryna Gurevych. Adapterhub: A framework for adapting transformers. *arXiv preprint arXiv:2007.07779*, 2020.

- [47] Vladislav Lialin, Sherin Muckatira, Namrata Shivagunde, and Anna Rumshisky. Relora: High-rank training through low-rank updates. In *The Twelfth International Conference on Learning Representations*, 2023.
- [48] Xinyu Yang, Jixuan Leng, Geyang Guo, Jiawei Zhao, Ryumei Nakada, Linjun Zhang, Huaxiu Yao, and Beidi Chen. S^2 FT: Efficient, scalable and generalizable LLM fine-tuning by structured sparsity. In *The Thirty-eighth Annual Conference on Neural Information Processing Systems*, 2024.
- [49] Andi Han, Jiaxiang Li, Wei Huang, Mingyi Hong, Akiko Takeda, Pratik Jawanpuria, and Bamdev Mishra. Sltrain: a sparse plus low-rank approach for parameter and memory efficient pretraining. *arXiv preprint arXiv:2406.02214*, 2024.
- [50] Rui Pan, Xiang Liu, Shizhe Diao, Renjie Pi, Jipeng Zhang, Chi Han, and Tong Zhang. Lisa: Layerwise importance sampling for memory-efficient large language model fine-tuning. *arXiv preprint arXiv:2403.17919*, 2024.
- [51] Jiawei Zhao, Zhenyu Zhang, Beidi Chen, Zhangyang Wang, Anima Anandkumar, and Yuandong Tian. Galore: Memory-efficient llm training by gradient low-rank projection. *arXiv preprint arXiv:2403.03507*, 2024.
- [52] Yutong He, Pengrui Li, Yipeng Hu, Chuyan Chen, and Kun Yuan. Subspace optimization for large language models with convergence guarantees. *arXiv preprint arXiv:2410.11289*, 2024.
- [53] Yongchang Hao, Yanshuai Cao, and Lili Mou. Flora: Low-rank adapters are secretly gradient compressors. *arXiv preprint arXiv:2402.03293*, 2024.
- [54] Ziyu Jiang, Xuxi Chen, Xueqin Huang, Xianzhi Du, Denny Zhou, and Zhangyang Wang. Back razor: Memory-efficient transfer learning by self-sparsified backpropagation. *Advances in neural information processing systems*, 35:29248–29261, 2022.
- [55] Zhiyuan Yu, Li Shen, Liang Ding, Xinmei Tian, Yixin Chen, and Dacheng Tao. Sheared back-propagation for fine-tuning foundation models. In *Proceedings of the IEEE/CVF Conference on Computer Vision and Pattern Recognition*, pages 5883–5892, 2024.
- [56] Paulius Micikevicius, Sharan Narang, Jonah Alben, Gregory Diamos, Erich Elsen, David Garcia, Boris Ginsburg, Michael Houston, Oleksii Kuchaiev, Ganesh Venkatesh, et al. Mixed precision training. *arXiv preprint arXiv:1710.03740*, 2017.
- [57] Tim Dettmers, Artidoro Pagnoni, Ari Holtzman, and Luke Zettlemoyer. Qlora: Efficient finetuning of quantized llms. *Advances in Neural Information Processing Systems*, 36, 2024.
- [58] Hanqing Zhu, Zhenyu Zhang, Wenyan Cong, Xi Liu, Sem Park, Vikas Chandra, Bo Long, David Z Pan, Zhangyang Wang, and Jinwon Lee. Apollo: Sgd-like memory, adamw-level performance. *arXiv preprint arXiv:2412.05270*, 2024.
- [59] Sunghyeon Woo, Baeseong Park, Byeongwook Kim, Minjung Jo, Sejung Kwon, Dongsuk Jeon, and Dongsoo Lee. Dropbp: Accelerating fine-tuning of large language models by dropping backward propagation. *arXiv preprint arXiv:2402.17812*, 2024.

A Missing Proofs

In this section, we provide detailed proofs for Theorem 4.5. We first prove the following lemma.

Lemma A.1. *Under Assumptions 4.1-4.4, if $\beta_1 \in (0, 1)$, it holds that*

$$\begin{aligned} \sum_{t=0}^T \mathbb{E}[\|\mathbf{m}^t - \nabla f(\mathbf{x}^t)\|_2^2] &\leq \frac{2\|\mathbf{m}^0 - \nabla f(\mathbf{x}^0)\|_2^2}{\beta_1} + \frac{4L^2}{\delta\beta_1^2} \sum_{t=1}^T \|\mathbf{x}^t - \mathbf{x}^{t-1}\|_2^2 \\ &\quad + \left(1 - \frac{\delta}{2}\right) (1 + 6\beta_1) \sum_{t=1}^T \mathbb{E}[\|\nabla f(\mathbf{x}^t)\|_2^2] + 6T\beta_1\sigma^2. \end{aligned} \quad (15)$$

Proof. According to the update of momentum, we have

$$\mathbf{m}^t - \nabla f(\mathbf{x}^t) = (1 - \beta_1)(\mathbf{m}^{t-1} - \nabla f(\mathbf{x}^t)) + \beta_1(\hat{\mathbf{g}}^t - \nabla f(\mathbf{x}^t)).$$

Taking expectation we have

$$\begin{aligned} \mathbb{E}[\|\mathbf{m}^t - \nabla f(\mathbf{x}^t)\|_2^2] &= \mathbb{E}[\|(1 - \beta_1)(\mathbf{m}^{t-1} - \nabla f(\mathbf{x}^t)) + \beta_1(\mathbb{E}[\hat{\mathbf{g}}^t] - \nabla f(\mathbf{x}^t))\|_2^2] \\ &\quad + \beta_1^2 \mathbb{E}[\|\hat{\mathbf{g}}^t - \mathbb{E}[\hat{\mathbf{g}}^t]\|_2^2]. \end{aligned} \quad (16)$$

For the first term, applying Jensen's inequality yields

$$\begin{aligned} &\mathbb{E}[\|(1 - \beta_1)(\mathbf{m}^{t-1} - \nabla f(\mathbf{x}^t)) + \beta_1(\mathbb{E}[\hat{\mathbf{g}}^t] - \nabla f(\mathbf{x}^t))\|_2^2] \\ &\leq (1 - \beta_1) \mathbb{E}[\|\mathbf{m}^{t-1} - \nabla f(\mathbf{x}^{t-1}) - \nabla f(\mathbf{x}^t) + \nabla f(\mathbf{x}^{t-1})\|_2^2] + \beta_1 \mathbb{E}[\|\mathbb{E}[\hat{\mathbf{g}}^t] - \nabla f(\mathbf{x}^t)\|_2^2]. \end{aligned} \quad (17)$$

By Young's inequality, we have

$$\begin{aligned} \mathbb{E}[\|\mathbf{m}^{t-1} - \nabla f(\mathbf{x}^{t-1}) - \nabla f(\mathbf{x}^t) + \nabla f(\mathbf{x}^{t-1})\|_2^2] &\leq \left(1 + \frac{\delta\beta_1}{2}\right) \mathbb{E}[\|\mathbf{m}^{t-1} - \nabla f(\mathbf{x}^{t-1})\|_2^2] \\ &\quad + \left(1 + \frac{2}{\delta\beta_1}\right) \mathbb{E}[\|\nabla f(\mathbf{x}^t) - \nabla f(\mathbf{x}^{t-1})\|_2^2]. \end{aligned} \quad (18)$$

For the second term, applying Cauchy's inequality yields

$$\begin{aligned} \mathbb{E}[\|\hat{\mathbf{g}}^t - \mathbb{E}[\hat{\mathbf{g}}^t]\|_2^2] &\leq 3\mathbb{E}\|\hat{\mathbf{g}}^t - \mathbf{g}^t\|_2^2 + 3\mathbb{E}\|\mathbf{g}^t - \nabla f(\mathbf{x}^t)\|_2^2 + 3\mathbb{E}\|\nabla f(\mathbf{x}^t) - \mathbb{E}[\hat{\mathbf{g}}^t]\|_2^2 \\ &\leq 6(1 - \delta)\mathbb{E}[\|\nabla f(\mathbf{x}^t)\|_2^2] + 3(2 - \delta)\sigma^2, \end{aligned} \quad (19)$$

where the last inequality uses Assumption 4.3 and 4.4. Applying (17)(18)(19) to (16) and using Assumption 4.2 and 4.4, we obtain

$$\begin{aligned} \mathbb{E}[\|\mathbf{m}^t - \nabla f(\mathbf{x}^t)\|_2^2] &\leq \left(1 - \beta_1 \left(1 - \frac{\delta}{2}\right)\right) \mathbb{E}[\|\mathbf{m}^{t-1} - \nabla f(\mathbf{x}^{t-1})\|_2^2] + \frac{2L^2}{\delta\beta_1} \mathbb{E}[\|\mathbf{x}^t - \mathbf{x}^{t-1}\|_2^2] \\ &\quad + (\beta_1 + 6\beta_1^2)(1 - \delta)\mathbb{E}[\|\nabla f(\mathbf{x}^t)\|_2^2] + 3(2 - \delta)\beta_1^2\sigma^2. \end{aligned} \quad (20)$$

Summing (20) for $t = 1, 2, \dots, T$ yields (15). \square

Now we are ready to prove Theorem 4.5. We first restate the theorem below in Theorem A.2.

Theorem A.2. *Under Assumptions 4.1-4.4, if $\beta_1 \in (0, \delta/(24 - 12\delta))$ and $\eta \leq \min\{1/2L, \sqrt{(\delta\beta_1^2)/(8L^2)}\}$, CeLoRA with momentum SGD converges as*

$$\frac{1}{T+1} \sum_{t=0}^T \mathbb{E}[\|\nabla f(\mathbf{x}^t)\|_2^2] \leq \frac{4[f(\mathbf{x}^0) - \inf_{\mathbf{x}} f(\mathbf{x})]}{\delta\eta(T+1)} + \frac{4\|\mathbf{m}^0 - \nabla f(\mathbf{x}^0)\|_2^2}{\delta\beta_1(T+1)} + \frac{12\beta_1\sigma^2}{\delta}. \quad (21)$$

Proof. By Assumption 4.2, we have

$$\begin{aligned} f(\mathbf{x}^{t+1}) - f(\mathbf{x}^t) &\leq \langle \nabla f(\mathbf{x}^t), \mathbf{x}^{t+1} - \mathbf{x}^t \rangle + \frac{L}{2} \|\mathbf{x}^{t+1} - \mathbf{x}^t\|_2^2 \\ &= \left\langle \frac{\mathbf{m}^t}{2}, \mathbf{x}^{t+1} - \mathbf{x}^t \right\rangle + \left\langle \nabla f(\mathbf{x}^t) - \frac{\mathbf{m}^t}{2}, \mathbf{x}^{t+1} - \mathbf{x}^t \right\rangle + \frac{L}{2} \|\mathbf{x}^{t+1} - \mathbf{x}^t\|_2^2 \\ &= -\left(\frac{1}{2\eta} - \frac{L}{2}\right) \|\mathbf{x}^{t+1} - \mathbf{x}^t\|_2^2 + \frac{\eta}{2} \|\nabla f(\mathbf{x}^t) - \mathbf{m}^t\|_2^2 - \frac{\eta}{2} \|\nabla f(\mathbf{x}^t)\|_2^2. \end{aligned} \quad (22)$$

Taking expectation and summing (22) for $t = 0, 1, \dots, T$ yields

$$\begin{aligned} \inf_{\mathbf{x}} f(\mathbf{x}) - f(\mathbf{x}^0) &\leq \frac{\eta}{2} \sum_{t=0}^T \mathbb{E}[\|\nabla f(\mathbf{x}^t) - \mathbf{m}^t\|_2^2] - \left(\frac{1}{2\eta} - \frac{L}{2}\right) \sum_{t=0}^T \mathbb{E}[\|\mathbf{x}^{t+1} - \mathbf{x}^t\|_2^2] \\ &\quad - \frac{\eta}{2} \sum_{t=0}^T \mathbb{E}[\|\nabla f(\mathbf{x}^t)\|_2^2]. \end{aligned} \quad (23)$$

Applying Lemma A.1 to (23) and noting that $\beta_1 \in (0, \delta/(24 - 12\delta))$ implies $(1 - \delta/2)(1 + 6\beta_1) \leq 1 - \delta/4$, we obtain

$$\begin{aligned} \frac{1}{T+1} \sum_{t=0}^T \mathbb{E}[\|\nabla f(\mathbf{x}^t)\|_2^2] &\leq \frac{4[f(\mathbf{x}^0) - \inf_{\mathbf{x}} f(\mathbf{x})]}{\delta\eta(T+1)} + \frac{4\|\mathbf{m}^0 - \nabla f(\mathbf{x}^0)\|_2^2}{\delta\beta_1(T+1)} + \frac{12\beta_1\sigma^2}{\delta} \\ &\quad - \frac{4}{\delta\eta} \left(\frac{1}{2\eta} - \frac{L}{2} - \frac{2\eta L^2}{\delta\beta_1^2}\right) \sum_{t=0}^T \|\mathbf{x}^{t+1} - \mathbf{x}^t\|_2^2. \end{aligned} \quad (24)$$

Since $\eta \leq \min\{1/2L, \sqrt{(\delta\beta_1^2)/(8L^2)}\}$ implies $1/(4\eta) \geq L/2$ and $1/(4\eta) \geq (2\eta L^2)/(\delta\beta_1^2)$, (21) is a direct result of (24). \square